Neurobiology of Aging 35 (2014) 576–584

Contents lists available at ScienceDirect

Neurobiology of Aging

journal homepage: www.elsevier.com/locate/neuaging

Amyloid burden and neural function in people at risk for Alzheimer's Disease

Sterling C. Johnson [a,b,c,*], Bradley T. Christian [b,d], Ozioma C. Okonkwo [a,b], Jennifer M. Oh [a,b], Sandra Harding [a,b], Guofan Xu [b,e], Ansel T. Hillmer [d], Dustin W. Wooten [d], Dhanabalan Murali [d], Todd E. Barnhart [d], Lance T. Hall [e], Annie M. Racine [b], William E. Klunk [g], Chester A. Mathis [h], Barbara B. Bendlin [a,b], Catherine L. Gallagher [a,b], Cynthia M. Carlsson [a,b], Howard A. Rowley [b,e], Bruce P. Hermann [b,c], N. Maritza Dowling [a,b,f], Sanjay Asthana [a,b,c], Mark A. Sager [b,c]

[a] Geriatric Research Education and Clinical Center, Wm. S. Middleton Memorial VA Hospital, Madison, WI, USA
[b] Alzheimer's Disease Research Center, University of Wisconsin School of Medicine and Public Health, Madison, WI, USA
[c] Wisconsin Alzheimer's Institute, University of Wisconsin School of Medicine and Public Health, Madison, WI, USA
[d] Department of Medical Physics, University of Wisconsin School of Medicine and Public Health, Madison, WI, USA
[e] Department of Radiology, University of Wisconsin School of Medicine and Public Health, Madison, WI, USA
[f] Department of Biostatistics and Medical Informatics, University of Wisconsin School of Medicine and Public Health, Madison, WI, USA
[g] Department of Psychiatry, University of Pittsburgh School of Medicine, Pittsburgh, PA, USA
[h] Department of Radiology, University of Pittsburgh School of Medicine, Pittsburgh, PA, USA

ARTICLE INFO

Article history:
Received 16 January 2013
Received in revised form 10 September 2013
Accepted 19 September 2013
Available online 23 October 2013

Keywords:
Alzheimer's disease
Amyloid imaging
Cognitive function
Glucose metabolism
AD risk

ABSTRACT

To determine the relationship between amyloid burden and neural function in healthy adults at risk for Alzheimer's Disease (AD), we used multimodal imaging with [C-11]Pittsburgh compound B positron emission tomography, [F-18]fluorodeoxyglucose, positron emission tomography , and magnetic resonance imaging, together with cognitive measurement in 201 subjects (mean age, 60.1 years; range, 46–73 years) from the Wisconsin Registry for Alzheimer's Prevention. Using a qualitative rating, 18% of the samples were strongly positive Beta-amyloid (Aβ+), 41% indeterminate (Aβi), and 41% negative (Aβ−). Aβ+ was associated with older age, female sex, and showed trends for maternal family history of AD and APOE4. Relative to the Aβ− group, Aβ+ and Aβi participants had increased glucose metabolism in the bilateral thalamus; Aβ+ participants also had increased metabolism in the bilateral superior temporal gyrus. Aβ+ participants exhibited increased gray matter in the lateral parietal lobe bilaterally relative to the Aβ− group, and no areas of significant atrophy. Cognitive performance and self report cognitive and affective symptoms did not differ between groups. Amyloid burden can be identified in adults at a mean age of 60 years and is accompanied by glucometabolic increases in specific areas, but not atrophy or cognitive loss. This asymptomatic stage may be an opportune window for intervention to prevent progression to symptomatic AD.

Published by Elsevier Inc.

1. Introduction

Beta-amyloid (1–42) (Aβ42) accumulation, a hallmark feature of Alzheimer's disease (AD), is putatively a major cause of neural dysfunction (Palop and Mucke, 2010) and eventual cognitive decline to dementia (Hardy and Higgins, 1992). The first major stage of presymptomatic AD might be a period of brain Aβ42 accumulation denoted by a positive amyloid positron emission tomography (PET) scan or abnormal levels of Aβ in the cerebrospinal fluid (CSF) (Sperling et al., 2011). A subset of healthy older adults have substantial amyloid burden in the brain when measured with amyloid PET imaging and associations with poorer cognitive function have been observed (Lim et al., 2012; Mathis et al., 2013; Rodrigue et al., 2012; Sperling et al., 2013). Because amyloid PET labels extracellular insoluble aggregates, a presumed reason for associations with cognition is via cumulative neurotoxicity resulting in eventual cognitive decline (Jack et al., 2011a). The specifics of the hypothesized model (Sperling et al., 2011) of preclinical amyloid staging are being elucidated empirically (Jack et al., 2011b, 2012; Jagust et al., 2012; Knopman et al., 2012, 2013), but the temporal relationship between amyloid burden and neural and cognitive dysfunction in the earliest stages of preclinical AD is complex (Bateman et al., 2012; Reiman et al., 2012), and causality is incompletely understood (Chetelat, 2013). An important model for studying disease

* Corresponding author at: William S. Middleton Memorial VA Hospital, 2500 Overlook Terrace (11G), GRECC, Madison, WI 53705, USA. Tel.: +1 608 256 1901 x11946; fax: +1 608 280 7165.
E-mail address: scj@medicine.wisc.edu (S.C. Johnson).

0197-4580/$ – see front matter Published by Elsevier Inc.
http://dx.doi.org/10.1016/j.neurobiolaging.2013.09.028

course in presymptomatic AD is to examine people who harbor risk factors for the disease. Other than age, having a first-degree relative (Okonkwo et al., 2012a; Sager et al., 2005; Xiong et al., 2011) and possessing the epsilon4 allele of the apolipoprotein E gene (APOE4) are by far the most substantive risk factors for AD and these have been associated with Aβ42 load and earlier age of Aβ42 accumulation using imaging methods (Fleisher et al., 2013; Morris et al., 2010; Mosconi et al., 2013; Rowe et al., 2010; Xiong et al., 2011). In the present study, the effect of amyloid burden on neural function in a subset of a cognitively healthy at-risk cohort known as the Wisconsin Registry for AD Prevention (WRAP) was examined. The cohort consisted of >1500 persons aged 40–65 at study entry enriched with parental family history and APOE4 who were followed serially (Sager et al., 2005). A major goal was to examine the rate of amyloid positivity (Aβ+) and its associated demographic, cognitive, and imaging characteristics in this sample. We hypothesized that Aβ+ would be associated with risk factors for AD, and with signs of neural dysfunction measured using glucometabolic imaging, volumetric gray matter atrophy, and cognition.

2. Methods

Two hundred and one adults were recruited from the WRAP registry either by in-person invitation at their main WRAP study visit or by mailed invitation. The mean age was 60.1 years (SD = 5.9 years), mean years of education was 16.1 (SD = 2.3), and 139 (67%) were women. Fifty-nine (29%) individuals reported no family history (FH) of AD; 95 (46%) had a maternal history of AD (mFH+); 44 (21%) had a paternal history (pFH+), and 9 (4%) had both parents afflicted with AD (mpFH+). APOE genotype was as follows: APOE e2/e2 = 0; e2/e3 = 23; e2/e4 = 7; e3/e3 = 96; e3/e4 = 69; e4/e4 = 6. The characteristics of this study sample did not differ significantly from the larger WRAP registry.

The method for determining the presence or absence of AD in the parent has been described previously (La Rue et al., 2008; Sager et al., 2005). The University of Wisconsin Institutional Review Board approved all study procedures and each subject provided signed informed consent before participation.

2.1. Imaging methods

The procedures involved undergoing a [C-11]Pittsburgh compound B ([C-11]PiB) positron emission tomography (PET) scan, an Fluorodeoxyglucose ([F-18] FDG PET) scan, (both on a the same Siemens EXACT HR+ scanner and typically occurring the same day), and a 3.0 Tesla magnetic resonance imaging (MRI) scan.

2.1.1. [C-11]PiB radiochemical synthesis

[C-11]PiB was synthesized using a captive solvent method (Wilson et al., 2000). N-methylation of the 2-(4′-amino-phenyl)-6-OH-benzothiazole (6-OH-BTA-0) precursor (ABX, Inc, Radeberg, Germany) was accomplished using [C-11] methyl triflate produced via an automated chemistry module and subsequently purified using high-performance liquid chromatography. Typical yields of final [C-11]PiB product were in excess of 2 GBq, with specific activities of 150–600 GBq/μmol. [F-18] FDG was purchased from a commercial vendor.

2.1.2. PiB PET scanning

The [C-11]PiB PET data were acquired in 3-D mode. Participants were positioned head first, supine with the canthomeatal line parallel to the in-plane field of view. A 6 minute transmission scan was acquired for attenuation correction. A 70-minute dynamic [C-11]PiB PET acquisition was then initiated with the injection of a 15 mCi target dose of [C-11]PiB bolus (mean 15.3 mCi, SD = 0.9), injected over 30 seconds. Dynamic acquisition frames included 5 × 2 minutes and 12 × 5 minutes for a total of 17 time frames. The PET data were reconstructed using a filtered back-projection algorithm (Direct inverse Fourier Transformation; DIFT) with sinogram trimming to a voxel size of 2.57 mm × 2.57 mm × 2.43 mm and matrix dimension of 128 × 128 × 63 and corrected for random events, attenuation of annihilation radiation, dead time, scanner normalization, and scatter radiation using the ECAT v7.2.2 software with segmented attenuation correction. The reconstructed time series of PET data were realigned using SPM8 (www.fil.ion.ucl.ac.uk/spm) to correct for subject motion during the course of the study and a denoising algorithm was applied to the voxel-based time series (Christian et al., 2010; Floberg et al., 2012). The PET time series was coregistered into the space defined according to the T1-weighted MRI scan based on coregistration with the time-integrated (i.e., sum image) [C-11] PET scan using mutual information.

2.1.3. Distribution volume ratio maps

The data were then transformed into voxel-wise parametric images representing [C-11]PiB binding using the cerebellar cortex as a reference region of negligible binding (Price et al., 2005). The cerebellar time–activity curve was extracted from the PET data using a cerebellar gray matter (GM) mask image derived from the coregistered T1-weighted MRI using FreeSurfer 5.3 software (http://surfer.nmr.mgh.harvard.edu/). Voxel-based parametric images using Logan graphical analysis were created as described previously (Lopresti et al., 2005). For the Logan graphical method (Logan et al., 1996), linear regression was applied to the transformed data using the 35–70 minute (7 points) interval and a mean efflux constant of 0.149/min. The resulting distribution volume ratio (DVR) images were each inspected for quality and rated for amyloid burden using a rating system described in (Section 2.1.4). Using SPM8, the DVRs were also spatially normalized to the International Consortium for Brain Mapping 152 atlas (ICBM 152, i.e., Montreal Neurological Institute [MNI] space) and smoothed with an 8-mm full width at half maximum Gaussian kernel and entered into voxel-wise group analyses.

2.1.4. Qualitative PiB rating

A qualitative score for amyloid burden was used for greater clinical applicability and to allow for the possibility of regional heterogeneity in this age range when amyloid burden may only be emerging. The visual rating of PiB positivity was achieved on the native space DVR images that were all scaled uniformly from 0.0 to 2.0, and displayed using a color map (the ACTC activation color map) that provided distinct shades of color for demarcating PiB positivity (approximately 1.2 or greater). After establishing high inter- and intrarater reliability (intraclass correlation coefficients of 0.95 and 0.96, respectively) on a set of 33 consecutively selected examinations, the entire set of examinations was rated in 1 session by a single rater (SCJ) blind to subject characteristics. Examinations were rated on a 4-point scale, where 0 represented no cortical amyloid burden or only nonspecific white matter uptake; 1 represented non-significant patchy or diffuse cortical GM binding not resembling an AD pattern (significant uptake in the basal ganglia was common and not considered in the amyloid score); 2 represented an indeterminate (Aβi) classification where GM binding was present in the cortex of at least 3 lobes resembling an AD disease pattern but less intense than an overtly positive scan; 3 represented unambiguous positive amyloid binding in the cortex (Aβ+). Category 0 occurred rarely (9 cases, too few to study as its own class) so 0 and 1 ratings were subsequently combined to form an amyloid negative (Aβ−) group. Fig. 1 depicts the rating categories with examples.

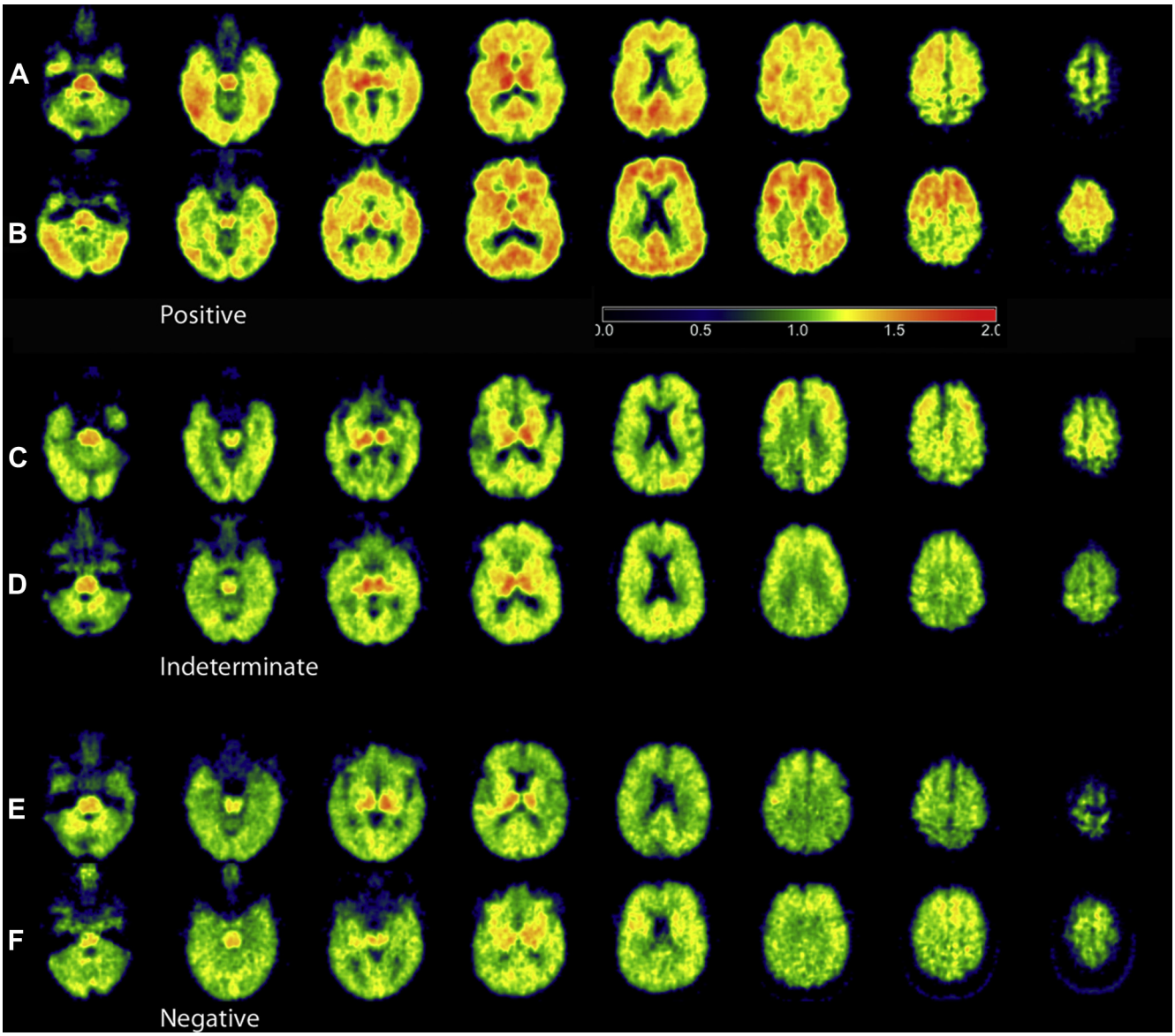

Fig. 1. Example Pittsburgh compound B (PiB) scans that were classified according to the rating system explained in the Methods. Shown are 6 participants who were classified as PiB Aβ-positive (A–B), indeterminate (C–D), and negative (E–F). All images are [C-11]PiB distribution volume ratio (DVR) maps and are displayed here using the ACTC color lookup table and scaled uniformly from 0.0 to 2.0 according to the inset color bar. The ages of these participants are 62, 54, 53, 67, 64, and 62 years, respectively, from top to bottom. Abbreviations: DVR, distribution volume ratio; PiB, Pittsburgh compound B.

2.1.5. FDG PET image formation and postprocessing

FDG PET imaging used the Alzheimer's Disease NeuroImaging Initiative protocol (Jagust et al., 2010) including 5 mCi FDG injection with a 30-minute uptake period and 30 minute transaxial acquisition. Post-processing involved frame-to-frame realignment and summation of the 30 minute emission scans, which were then coregistered to the T1-weighted MRI scan. The images were spatially normalized to the ICBM 152 atlas and smoothed to 8 mm using SPM8 and subsequently entered into statistical analyses. Intensity normalization was achieved by calculating the mean signal over the pons and cerebellar vermis (Jagust et al., 2012; Knopman et al., 2013) and including this value in the statistical analysis using the ANCOVA normalization option in SPM8.

2.1.6. MRI protocol

All participants were scanned using a GE 3.0 Tesla MR750 (Waukesha, WI, USA) using an 8 channel head coil. A T1-weighted brain volume was acquired in the axial plane with a 3-D inversion recovery prepared fast spoiled gradient-echo sequence using the following parameters: inversion time (TI) = 450 ms; repetition time (TR) = 8.1 ms; echo time (TE) = 3.2 ms; flip angle = 12°; acquisition matrix = 256 × 256 × 156 mm, field of view (FOV) = 256 mm; slice thickness = 1.0 mm. Voxels were 1 mm isotropic. The image acquisition protocol also included T2-weighted and fluid attenuated inversion recovery (FLAIR) anatomical scans, which were reviewed by a neuroradiologist (HAR) for exclusionary abnormalities. The T1-weighted volume was segmented into tissue classes using the new segment feature in SPM8 and the resulting modulated and spatially normalized GM probability maps were smoothed to 8 mm Gaussian and entered into statistical analysis.

2.2. Neuropsychological assessment

Participants completed a comprehensive neuropsychological battery (Sager et al., 2005) proximal to the time of scanning that

included a global cognitive measure (Mini Mental State Examination) and domain-specific tests. The battery included but was not limited to tests shown in Table 1. The tests selected for inclusion in analyses emphasized memory, executive function, and self-report measures of cognitive and mood symptoms.

2.3. Statistical analysis

Demographic and neuropsychological data were analyzed using SPSS 20.0 (IBM Corp, Armonk, NY, USA) with Aβ ratings as the group factor. Categorical variables were analyzed using χ^2 tests; continuous variables were analyzed using 1-way analysis of variance (ANOVA). The analysis of neuropsychological measures was done using a series of 1-way ANCOVAs with amyloid group status as a fixed factor and age, education, sex, parental FH of AD, and APOE4 genotype as covariates (FH and APOE4 were binary variables for presence/absence of the characteristic).

2.3.1. Imaging analyses

Univariate ANCOVA was conducted on imaging modalities with Aβ ratings as the group factor. Analyses were conducted with SPM8. A descriptive analysis of the PiB images was done first, without any covariates to simply describe the spatial regions where the groups differed. This was followed by inferential voxel-wise tests on measures of neural function as approximated by FDG. An omnibus *F* test for group differences was conducted followed by post hoc contrasts to further interrogate significant regions in the *F* test. GM was quantified using voxel-based morphometry (VBM) segmentation and statistical methods (Ashburner and Friston, 2000). In all of these analyses of metabolism and volume, the search region and inference were constrained to GM of the cerebrum only, which was achieved by binarizing the SPM canonical GM a priori probability map at 0.3 multiplied by a binary map of the left and right cerebral hemispheres from the Wake Forest Pick Atlas (Maldjian et al., 2003). For each model we included APOE4 status (binary variable), FH of AD, sex, and age as covariates. The FH covariate was treated as a binary covariate because subgroup categories (maternal, paternal, both, neither) are not known to be ordinal. For the GM VBM analysis, total intracranial volume was also a covariate. Covariates were mean-centered. Inference was based on familywise error (FWE) multiple comparison correction using random field theory (Worsley et al., 2004). For FDG this entailed initially passing through a voxel level threshold of $p < 0.005$ together with cluster extent >100 voxels and FWE-corrected *p*-values are reported for the voxel and cluster level in GM of the cerebrum among only those voxels surviving the *F* test ($p = 0.005$ threshold). For VBM, the same procedures were used, and inference was at the voxel-level because of non-stationarity (Ridgway et al., 2008). Correlations of amyloid load with age were computed using Pearson correlation coefficients. The amyloid variable was not distributed normally and was therefore transformed to a normal shape using a rank-based inverse normal (Rankit) transformation. Correlations on both the raw and transformed data were performed. Nonparametric Spearman correlations were also computed on the raw data. For these correlations, the amyloid values were derived from 6 regions of space were defined a priori based on significant group differences observed in 12 amnestic mild cognitive impairment (MCI) patients (mean age 71.8, SD = 10.0; 5 women, 7 men) with presumed AD etiology diagnosed in a multidisciplinary consensus conference of the Wisconsin Alzheimer's Disease Research Center using standard criteria (Albert et al., 2011), and compared with 12 matched control subjects (mean age 68.1, SD = 10.9; 8 women, 4 men) who underwent the same [C11]PiB acquisition and processing protocol as the main sample. The regions included 4-mm spheres around peak maxima in the posterior cingulate (MNI coordinates −6, −54, 30), orbital frontal (6, 46, −4), left and right

Table 1
Baseline characteristics of participants ($n = 201$)[a]

Variable	Amyloid negative, ($n = 83$)	Amyloid indeterminate, ($n = 82$)	Amyloid positive, ($n = 36$)	p[b]
Demographic characteristic				
FH positive, %	69.9	67.1	83.3	0.189
Maternal FH positive, %	41.0	42.7	63.9	0.054
APOE4 positive, %	38.6	35.4	55.6	0.110
Female, %	54.2	75.6	77.8	0.005
Age at PiB scan	59.33 (5.67)	60.05 (6.16)	62.78 (4.33)	0.010
Education	16.04 (2.38)	16.01 (2.34)	16.50 (2.35)	0.548
Interval between PiB scan and cognitive testing (in months)	7.49 (7.05)	7.60 (6.55)	8.74 (9.56)	0.677
Clinical/Cognitive				
MMSE	29.19 (1.09)	29.39 (1.09)	29.28 (1.14)	0.527
RAVLT total	49.67 (7.83)	52.40 (7.61)	51.57 (7.98)	0.077
RAVLT long delay	10.39 (2.82)	10.72 (2.72)	10.30 (2.88)	0.657
BVMT-R total	24.43 (5.92)	24.70 (5.80)	25.21 (6.06)	0.819
BVMT-R delay	9.48 (2.28)	9.41 (2.17)	9.22 (2.28)	0.857
COWAT	47.75 (11.30)	44.32 (11.05)	46.68 (11.52)	0.582
WAIS digit span total	17.80 (4.28)	17.77 (4.26)	17.61 (4.38)	0.977
Trail making test A	26.02 (7.20)	25.73 (7.07)	26.67 (7.38)	0.813
Trail making test B	60.65 (19.95)	63.18 (19.57)	58.97 (20.34)	0.512
Stroop color-word	111.38 (17.67)	109.40 (17.30)	106.42 (18.00)	0.397
WCST perseverative response	8.20 (6.38)	7.59 (6.25)	6.23 (6.54)	0.339
IQCODE	47.36 (5.65)	47.42 (5.53)	48.60 (5.76)	0.527
Memory self rating	4.90 (1.18)	4.99 (1.18)	4.74 (1.20)	0.560
CES-D	5.73 (6.19)	5.91 (6.07)	5.91 (6.36)	0.981

Key: *APOE4,* the epsilon 4 allele of the apolipoprotein E gene; BVMT-R, Brief Visuospatial Memory Test-Revised; CES-D, Center for Epidemiologic Studies Depression Scale; COWAT, the Controlled Oral Word Association Test, C-F-L version; FH, family history of Alzheimer's disease; IQCODE, Informant Questionnaire on Cognitive Decline in the Elderly; MMSE, Mini-Mental State Exam; PiB, Pittsburgh compound B; RAVLT, Rey Auditory Verbal Learning Test; WAIS, Wechsler Adult Intelligence Scale; WCST, Wisconsin Card Sort Test.

[a] All values are mean (SD) except where otherwise indicated.

[b] Reported *p* value is for omnibus test of group difference.

lateral temporal lobe (−60, −60, 0, and 58, −60, −8), and left and right lateral parietal lobes (−46, −64, 34 and 50, −60, 40).

3. Results

Table 1 presents demographic and cognitive data according to Aβ positivity groupings. Eighteen percent of the samples were strongly Aβ+, 41% were classified as Aβi (indeterminate), and 41% were Aβ−. The Aβ+ group was significantly ($p = 0.01$) older (by 3.5 years) than the Aβ− group. The Aβi and Aβ+ groups contained a significantly greater proportion of women than the Aβ− group ($p = 0.005$). The Aβ+ group tended to be comprised of a greater proportion of maternal FH (64% in the amyloid positive group vs. 41% and 43% in the Aβi and Aβ− groups; $p = 0.054$). APOE4 status was not different between groups although a trend ($p = 0.11$) was also evident in this already enriched cohort.

3.1. Patterns of amyloid deposition

The spatial locations where the Aβi and Aβ+ groups differed from the Aβ− group are shown in Fig. 2. These effects were strongly significant using a FWE-corrected p-value (p_c) of 0.05 and were in regions typically seen in AD including the cortex of the medial and lateral parietal lobe, anterior medial and lateral frontal lobe, and lateral temporal lobe. Because the amyloid ratings defined the groups, differences were expected and are presented descriptively to show regions where amyloid load occurred.

3.2. Age and amyloid burden

The age effect was examined further in 6 regions of interest (posterior cingulate/precuneus, lateral temporal cortex bilaterally, lateral parietal cortex bilaterally, and medial frontal pole) and 2 of these regions are shown in Fig. 3 where quantitative amyloid burden in each region is scatter-plotted against age. Because the PiB distribution on age was skewed, we applied a rank-based normalizing transform to the PiB region of interest distributions and fitted a least squares regression line (also shown in Fig. 3). The

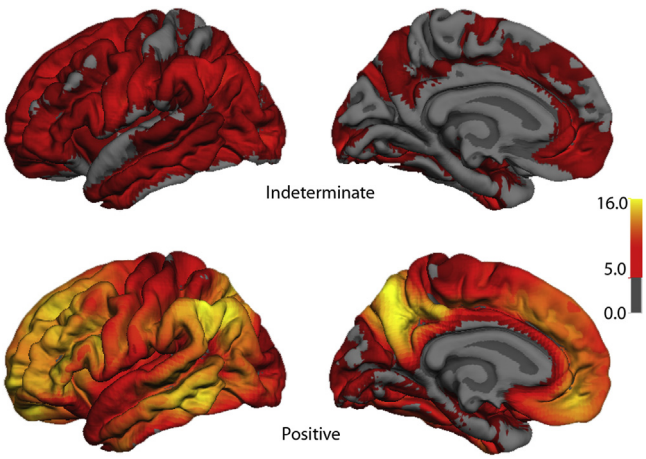

Fig. 2. Spatial location of amyloid positivity in subjects rated as beta-amyloid intermediate (Aβi) and beta-amyloid positive (Aβ+) versus subjects rated as beta-amyloid negative (Aβ−). Top row: Left lateral and medial renderings with color overlay of the statistical map where the Aβi group has more amyloid load than the Aβ− group. Bottom row: Left lateral and medial views where the Aβ+ group exhibited significantly more amyloid load than the Aβ− group. Color bar represents the value of the t-statistic. The minimum t value in these maps is t = 5.0 which exceeds the voxel-level family wise error correction threshold. Abbreviations: Aβi, beta-amyloid intermediate; Aβ−, beta-amyloid negative; Aβ+, beta-amyloid positive.

Pearson correlations (on the raw region of interest data) with age were as follows: posterior cingulate $r = 0.20$, $p = 0.004$; left lateral temporal cortex $r = 0.25$, $p < 0.001$; right lateral temporal lobe $r = 0.31$, $p < 0.001$; left lateral parietal cortex $r = 0.23$, $p = 0.002$; right lateral parietal cortex $r = 0.24$, $p = 0.001$; medial frontal cortex $r = 0.14$, $p = 0.05$. Pearson correlations on the transformed PiB variables and correlations using Spearman ρ coefficients on the raw data were also computed with nearly identical results. These correlations suggest a moderate relationship between age and PiB load in this age range.

3.3. Glucose metabolism according to amyloid load

To determine whether severity of amyloid burden was associated with neural function we examined glucose metabolism with FDG uptake and computed an ANOVA in which the amyloid rating was the grouping variable and FDG uptake the dependent variable. An omnibus F test for any group differences was first computed followed by simple effects (computed among only those voxels significant on the Ftest) to ascertain which groups were different and the direction of the effect. The Aβi group exhibited greater metabolism relative to the Aβ− group in the medial thalamus (−4, −18, 2; $t = 5.25$, FWE voxel $p_c < 0.001$, $k = 1226$; cluster-level $p_c = 0.003$) and left lateral prefrontal cortex (−36, 26, 32; $t = 4.26$, $p_c = 0.008$, $k = 343$, cluster $p_c = 0.09$). The Aβ+ group exhibited greater metabolic activity relative to the Aβ− group in the medial thalamus bilaterally (−4, −20, 0; $t = 4.13$, voxel $p_c = 0.014$, $k = 1272$, cluster $p_c = 0.002$) and the superior temporal gyrus bilaterally (left −44, −20,4; $t = 4.33$, voxel $p_c = 0.007$, $k = 282$, cluster $p_c = 0.123$; right 58, −6, −4; $t = 3.74$, $p_c = 0.05$, $k = 165$ cluster $p_c = 0.229$). These are shown in Fig. 4. There were no regions where the Aβ+ and Aβi groups exhibited significantly less FDG metabolism relative to the Aβ− group.

3.4. Gray matter volume by amyloid load

A 3-group ANOVA was computed voxelwise on 188 participants. There were no regions where the Aβ+ group exhibited lower volume than the Aβ− group. In contrast, the Aβ+ group exhibited greater GM volume in the lateral parietal lobe bilaterally (right: 33, −43, 54; $t = 4.38$, $p < 0.001$, 1010 voxels; left: −34, −42, 52, $t = 3.83$, $p < 0.001$, 529 voxels) and right ventral temporal lobe (48, −40, −21, $t = 4.12$, $p < 0.001$, 1107 voxels). However, none of these differences reached voxel-level significance when corrected for multiple comparisons.

3.5. Cognitive function by amyloid load

Several cognitive measures were compared in 3 groups using ANCOVA. Because cognitive performance can be affected by age, education, and sex, these were included as covariates. Binary variables for positive parental family history and APOE4 genotype were also included as covariates. Means and standard deviations are shown in Table 1 together with the p-value of the F statistic. Groups did not differ on any of the cognitive measures. Nor did they differ on subjective cognitive complaints or symptoms of depression.

4. Discussion

In vivo amyloid imaging with compounds such as [C-11]PiB may have utility in detecting preclinical AD at a time when intervention may be optimal. Here our purpose was to examine the demographic, cognitive, and imaging characteristics of subjects who differed in amyloid load among a relatively younger

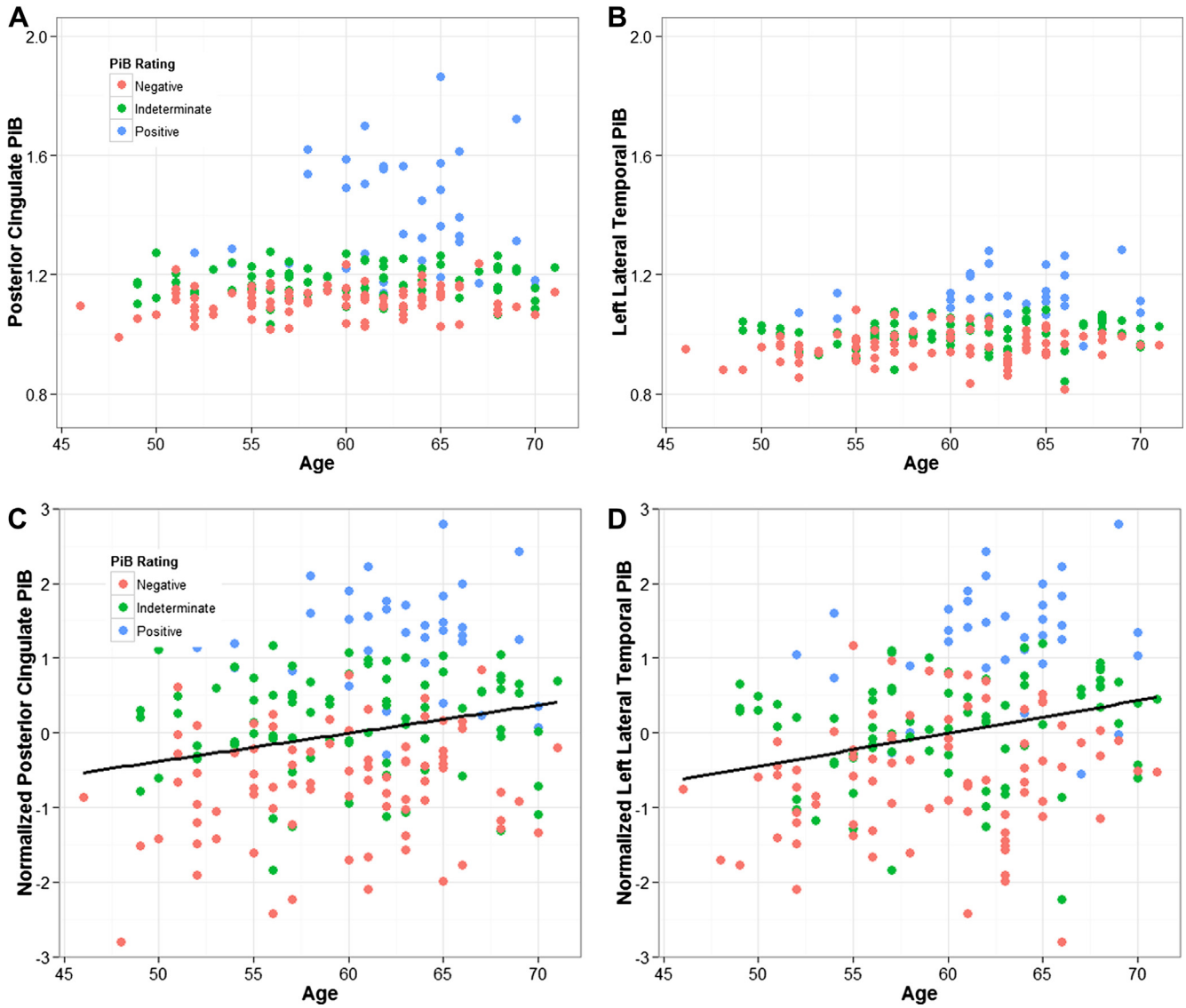

Fig. 3. Scatter plot of age by amyloid burden in selected regions of interest including (A) the posterior cingulate (MNI coordinate −6, −54, 30) and (B) left lateral temporal cortex (−60, −60, 0). Transformed Pittsburgh compound B (PiB) region of interest (ROI) distributions were also computed and plotted in C and D on age together with the least squares regression line. Amyloid group classifications of Aβ− (red), Aβi (green) and Aβ+ (blue) are shown for reference. Abbreviations: PiB, Pittsburgh compound B; ROI, region of interest.

cohort of subjects with a mean age of 60. In this study we found that 18% of people in the WRAP longitudinal cohort (which is enriched with persons who have parental FH of AD and APOE4 genotype) were strongly positive for amyloid. The areas of amyloid load were those that are typically seen in people with AD. The Aβ+ group was 3 years older and had a disproportionately greater representation of women. Trends were observed for maternal FH and APOE4 status. At this relatively young age,

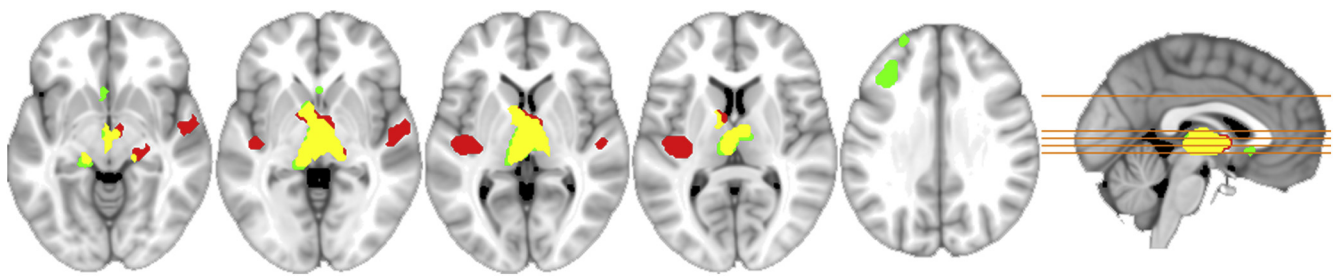

Fig. 4. Fluorodeoxyglucose (FDG) group differences: regions where the Aβ+ (red) and Aβi (green) groups exhibited significantly higher FDG uptake compared with the Aβ− group. Areas in yellow depict overlapping results. There were no regions where the Aβ+ and Aβi groups had significantly less uptake compared with the Aβ− group. The result maps are displayed on axial slices of a template image from inferior to superior at MNI z-coordinates: −7, −2, 3, 8, and 32. A mid-sagittal reference image is also shown depicting the elevations of the axial slices. Left is on left. Abbreviation: FDG, fluorodeoxyglucose.

amyloid positivity was not accompanied by lower GM volume, or cognition; nor did groups differ on subjective cognitive or mood symptoms, suggesting that Aβ+ subjects may be in a preclinical epoch. Glucose metabolism was greater in thalamus bilaterally in the Aβi and Aβ+ groups relative to the Aβ− group and higher bilaterally (again relative to the Aβ− group) in the lateral temporal lobe of the Aβ+ group.

The magnitude of the positive relationship between amyloid load and age (mean age 60 years; range 46–73 years) was significant although moderate (simple correlations between 0.20 and 0.30 in temporal and parietal cortices) and the values we report are slightly lower than values recently reported in a healthy adult sample not enriched for AD risk factors and spanning a broader age range of 30–89 (Rodrigue et al., 2012). Our finding of 18% amyloid positivity is generally consistent, if not slightly higher, than (Rowe et al., 2010) who found 10% positivity in healthy adults aged 50–59 and 18% positivity in healthy adults aged 60–69. Morris et al. 2010 found approximately 19% Aβ+ in adults aged 60–69 and 4.5% in adults aged 45–59 (in that sample, PiB load in each age group differed by APOE4 status). Amyloid positivity increases with age among normal subjects in the Alzheimer's Disease NeuroImaging Initiative and Australian Imaging, Biomarkers and Lifestyle cohort studies (Jagust et al., 2010; Rowe et al., 2010). The effect of sex was also significant. A previous study in older normal subjects (not enriched for AD risk) did not find a sex effect (Mielke et al., 2012). It is known that the effect of APOE4 on risk for AD is greater in women (Farrer et al., 1997).

The Aβ+ group tended to have a greater rate of maternal family history of AD ($p = 0.054$). This trend is consistent with recent reports (Mosconi et al., 2010, 2013) in which greater amyloid burden in healthy older adults with maternal FH was described. This is also consistent with reports in which it was suggested that maternal FH is associated with lower cerebral blood flow (Okonkwo et al., 2012b), lower metabolic rate of glucose (Mosconi et al., 2007, 2009), cerebral atrophy (Honea et al., 2010, 2011), and altered white matter microstructure on diffusion tensor imaging scans (Bendlin et al., 2010). Maternal inheritance of AD is significantly more common than paternal inheritance (Edland et al., 1996). The mechanism of this phenomenon is an active area of research (Swerdlow, 2011). The lack of a significant association with APOE genotype in this study is likely due to the young age of our sample and it may be that APOE associations are region-specific in a manner that was not tested with the design of this study. In other studies on older participants (Mathis et al., 2013; Mielke et al., 2012) and disease groups, significant associations have been found between amyloid load and APOE, and between glucose metabolism and APOE (for example, Jagust et al., 2012; Landau et al., 2012).

4.1. Amyloid load and neural function

The Aβi and Aβ+ group exhibited areas of greater FDG metabolism relative to the Aβ−- group and no areas of reduced metabolism. Among Aβi, the effect was predominant in the bilateral medial thalamus; whereas in Aβ+ greater metabolism was found in the medial thalamus and superior temporal gyrus bilaterally. Studies of FDG in people at risk (e.g. APOE status, FH status) have typically reported hypometabolism, rather than hypermetabolism. However, when subjects were grouped according to amyloid burden, increases in glucose metabolism associated with amyloid load have been observed. In a study of older healthy adults (mean age of 74), a positive relationship between global PiB burden and FDG metabolism in the posterior cingulate was observed (Oh et al., 2012). In another study a positive relationship was reportedamong MCI subjects in whom greater FDG metabolism in a precuneus region of interest was associated with greater PiB burden in medial and lateral parietal lobes and posterolateral temporal lobes bilaterally (Cohen et al., 2009). However, other studies do not agree (Knopman et al., 2013; Lowe et al., 2009). It is possible that the FDG differences we observed represent a higher basal metabolic rate in the amyloid positive subjects (Cohen et al., 2009). It may also be that this represents an early event in the AD cascade in reaction to the presence of amyloid, in a process that eventually leads to metabolic decline. This may be a compensatory response in distressed neural systems, a hypothesis that has been invoked in the functional imaging literature in people at risk to explain increased cerebral activation with increasing AD risk (Dickerson et al., 2004; Jacobs et al., 2012; Nichols et al., 2012). Longitudinal measurements in these subjects are needed to address this and are planned. It is intriguing that the hypermetabolic findings we observed are predominant in the thalamus. This is not typically viewed as an AD-vulnerable region, although it is now increasingly observed with amyloid imaging methods that this region commonly has high amyloid load (Furst and Lal, 2011; Mosconi et al., 2010).

4.2. Amyloid, gray matter volume, and cognition

The Aβ+ group exhibited no indications of atrophy in this cross-sectional study, but did exhibit bilateral parietal areas of increased volume relative to the Aβ− group. This finding was not significant when corrected for multiple comparisons. However, anatomic differences associated with amyloid burden are of interest and in at least 1 other study (Chetelat et al., 2010) larger volumes (in their case temporal lobe volumes) were reported in controls who were amyloid positive relative to amyloid negative controls. Studies of prospective volumetric change are planned in this cohort. Changes in white matter microstructure associated with amyloid in this relatively young at-risk population have not been assessed and are also planned including the analysis of white matter pathways that stem from the amyloid-rich regions we observed.

With regard to cognitive function, the 3 groups scored in the high normal range and did not differ on any of the measures including measures of verbal and visuospatial episodic learning and delayed recall, working memory, processing speed, and executive function. This is not surprising because the sample was relatively young and because there was only questionable evidence of neural injury (in the upregulated FDG results) that would be expected to precede cognitive decline (Sperling et al., 2011). The groups also did not differ on subjective cognitive complaints or endorsement of mood symptoms. Because the WRAP cohort is longitudinally followed, we will be able to examine trajectories of cognitive decline with regard to amyloid load and other brain imaging modalities as the study progresses.

The indeterminate amyloid group comprised 41% of the sample. This group is potentially of high interest because at least some of these subjects might begin to develop amyloid positivity (Chételat et al., 2013). The rating of an Aβi level of amyloid was based on the presence of GM PiB uptake in at least 3 lobes, but not sufficiently abundant to warrant an unambiguously positive rating. All subjects are being asked to return for repeat imaging in 2 years later to assess longitudinal progression in amyloid load and whether such a change is associated with other imaging or cognitive features.

The relationship between imaging markers of amyloid and cerebrospinal fluid (CSF) markers in this population is of particular relevance. Approximately 50% of the sample here agreed to donate CSF and studies designed to compare the concordance and predictive ability of these imaging and CSF markers are planned.

4.3. Conclusion

This study aimed to elucidate the rate of amyloid positivity and associated demographic, imaging, and cognitive findings among a cohort enriched for risk factors for AD. We have shown that a positive scan in this at-risk cohort is not related to concomitant decrements in cognition or cerebral atrophy, but was associated with area-specific increases in glucose metabolism suggestive of a period of reactive or compensatory signal that will be investigated further in a longitudinal study. The sample was highly educated, two-thirds female and predominantly Caucasian, potentially limiting the generalizability of the findings. Because amyloid signal is evident at least a decade before expected onset of MCI and AD cognitive symptoms (Sperling et al., 2011), these data join other studies to suggest that it is feasible to screen and enroll amyloid positive subjects into secondary prevention clinical trials that are implemented before neuronal degeneration and cognitive decline. Such a time window may be optimal for treatment effectiveness in delaying or preventing symptomatic AD.

Disclosure statement

The authors have no actual or potential conflicts of interest.

Acknowledgements

The authors thank Andrew Higgins, Caitlin Cleary, Amy Hawley, and staff at the Waisman Center for assistance with this project. This research was supported by NIA grants AG021155 (SCJ), AG027161 (MAS), and P50 AG033514 (SA); by a Veterans Administration Merit Review Grant I01CX000165 (SCJ); by P50 HD03352, and by a Clinical and Translational Science Award (UL1RR025011) to the University of Wisconsin, Madison. Portions of this research were supported by the Helen Bader Foundation, Northwestern Mutual Foundation, Extendicare Foundation, and from the Veterans Administration including facilities and resources at the Geriatric Research Education and Clinical Center of the William S. Middleton Memorial Veterans Hospital, Madison, WI.

References

Albert, M.S., DeKosky, S.T., Dickson, D., Dubois, B., Feldman, H.H., Fox, N.C., Gamst, A., Holtzman, D.M., Jagust, W.J., Petersen, R.C., Snyder, P.J., Carrillo, M.C., Thies, B., Phelps, C.H., 2011. The diagnosis of mild cognitive impairment due to Alzheimer's disease: recommendations from the National Institute on Aging-Alzheimer's Association workgroups on diagnostic guidelines for Alzheimer's disease. Alzheimers Dement. 7, 270–279.

Ashburner, J., Friston, K.J., 2000. Voxel-based morphometry—the methods. Neuroimage 11, 805–821.

Bateman, R.J., Xiong, C., Benzinger, T.L., Fagan, A.M., Goate, A., Fox, N.C., Marcus, D.S., Cairns, N.J., Xie, X., Blazey, T.M., Holtzman, D.M., Santacruz, A., Buckles, V., Oliver, A., Moulder, K., Aisen, P.S., Ghetti, B., Klunk, W.E., McDade, E., Martins, R.N., Masters, C.L., Mayeux, R., Ringman, J.M., Rossor, M.N., Schofield, P.R., Sperling, R.A., Salloway, S., Morris, J.C., 2012. Clinical and biomarker changes in dominantly inherited Alzheimer's disease. N. Engl. J. Med. 367, 795–804. http://dx.doi.org/10.1056/NEJMoa1202753.

Bendlin, B.B., Ries, M.L., Canu, E., Sodhi, A., Lazar, M., Alexander, A.L., Carlsson, C.M., Sager, M.A., Asthana, S., Johnson, S.C., 2010. White matter is altered with parental family history of Alzheimer's disease. Alzheimers Dement. 6, 394–403. http://dx.doi.org/10.1016/j.jalz.2009.11.003.

Chetelat, G., 2013. Alzheimer disease: Abeta-independent processes-rethinking preclinical AD. Nat. Rev. Neurol. 9, 123–124. http://dx.doi.org/10.1038/nrneurol.2013.21.

Chételat, G., La Joie, R., Villain, N., Perrotin, A., de La Sayette, V., Eustache, F., Vandenberghe, R., 2013. Amyloid imaging in cognitively normal individuals, at-risk populations and preclinical Alzheimer's disease. Neuroimage 2, 356–365. http://dx.doi.org/10.1016/j.nicl.2013.02.006.

Chetelat, G., Villemagne, V.L., Pike, K.E., Baron, J.C., Bourgeat, P., Jones, G., Faux, N.G., Ellis, K.A., Salvado, O., Szoeke, C., Martins, R.N., Ames, D., Masters, C.L., Rowe, C.C., Australian Imaging, B., Lifestyle Study of Ageing Research, G, 2010. Larger temporal volume in elderly with high versus low beta-amyloid deposition. Brain 133, 3349–3358. http://dx.doi.org/10.1093/brain/awq187.

Christian, B.T., Vandehey, N.T., Floberg, J.M., Mistretta, C.A., 2010. Dynamic PET denoising with HYPR processing. J. Nucl. Med. 51, 1147–1154. http://dx.doi.org/10.2967/jnumed.109.073999.

Cohen, A.D., Price, J.C., Weissfeld, L.A., James, J., Rosario, B.L., Bi, W., Nebes, R.D., Saxton, J.A., Snitz, B.E., Aizenstein, H.A., Wolk, D.A., Dekosky, S.T., Mathis, C.A., Klunk, W.E., 2009. Basal cerebral metabolism may modulate the cognitive effects of Abeta in mild cognitive impairment: an example of brain reserve. J. Neurosci. 29, 14770–14778. http://dx.doi.org/10.1523/JNEUROSCI.3669-09.2009.

Dickerson, B.C., Salat, D.H., Bates, J.F., Atiya, M., Killiany, R.J., Greve, D.N., Dale, A.M., Stern, C.E., Blacker, D., Albert, M.S., Sperling, R.A., 2004. Medial temporal lobe function and structure in mild cognitive impairment. Ann. Neurol. 56, 27–35.

Edland, S.D., Silverman, J.M., Peskind, E.R., Tsuang, D., Wijsman, E., Morris, J.C., 1996. Increased risk of dementia in mothers of Alzheimer's disease cases: evidence for maternal inheritance. Neurology 47, 254–256.

Farrer, L.A., Cupples, L.A., Haines, J.L., Hyman, B., Kukull, W.A., Mayeux, R., Myers, R.H., Pericak-Vance, M.A., Risch, N., van Duijn, C.M., 1997. Effects of age, sex, and ethnicity on the association between apolipoprotein E genotype and Alzheimer disease. A meta-analysis. APOE and Alzheimer Disease Meta Analysis Consortium. JAMA 278, 1349–1356.

Fleisher, A.S., Chen, K., Liu, X., Ayutyanont, N., Roontiva, A., Thiyyagura, P., Protas, H., Joshi, A.D., Sabbagh, M., Sadowsky, C.H., Sperling, R.A., Clark, C.M., Mintun, M.A., Pontecorvo, M.J., Coleman, R.E., Doraiswamy, P.M., Johnson, K.A., Carpenter, A.P., Skovronsky, D.M., Reiman, E.M., 2013. Apolipoprotein E epsilon4 and age effects on florbetapir positron emission tomography in healthy aging and Alzheimer disease. Neurobiol. Aging 34, 1–12. http://dx.doi.org/10.1016/j.neurobiolaging.2012.04.017.

Floberg, J.M., Mistretta, C.A., Weichert, J.P., Hall, L.T., Holden, J.E., Christian, B.T., 2012. Improved kinetic analysis of dynamic PET data with optimized HYPR-LR. Med. Phys. 39, 3319–3331. http://dx.doi.org/10.1118/1.4718669.

Furst, A.J., Lal, R.A., 2011. Amyloid-beta and glucose metabolism in Alzheimer's disease. J. Alzheimers Dis. 26 (Suppl 3), 105–116. http://dx.doi.org/10.3233/JAD-2011-0066.

Hardy, J.A., Higgins, G.A., 1992. Alzheimer's disease: the amyloid cascade hypothesis. Science 256, 184–185.

Honea, R.A., Swerdlow, R.H., Vidoni, E.D., Goodwin, J., Burns, J.M., 2010. Reduced gray matter volume in normal adults with a maternal family history of Alzheimer disease. Neurology 74, 113–120. http://dx.doi.org/10.1212/WNL.0b013e3181c918cb.

Honea, R.A., Swerdlow, R.H., Vidoni, E.D., Burns, J.M., 2011. Progressive regional atrophy in normal adults with a maternal history of Alzheimer disease. Neurology 76, 822–829. http://dx.doi.org/10.1212/WNL.0b013e31820e7b74.

Jack Jr., C.R., Albert, M.S., Knopman, D.S., McKhann, G.M., Sperling, R.A., Carrillo, M.C., Thies, B., Phelps, C.H., 2011a. Introduction to the recommendations from the National Institute on Aging-Alzheimer's Association workgroups on diagnostic guidelines for Alzheimer's disease. Alzheimers Dement. 7, 257–262. http://dx.doi.org/10.1016/j.jalz.2011.03.004.

Jack Jr., C.R., Vemuri, P., Wiste, H.J., Weigand, S.D., Aisen, P.S., Trojanowski, J.Q., Shaw, L.M., Bernstein, M.A., Petersen, R.C., Weiner, M.W., Knopman, D.S., 2011b. Evidence for ordering of Alzheimer disease biomarkers. Arch. Neurol. 68, 1526–1535. http://dx.doi.org/10.1001/archneurol.2011.183.

Jacobs, H.I., Van Boxtel, M.P., Heinecke, A., Gronenschild, E.H., Backes, W.H., Ramakers, I.H., Jolles, J., Verhey, F.R., 2012. Functional integration of parietal lobe activity in early Alzheimer disease. Neurology 78, 352–360. http://dx.doi.org/10.1212/WNL.0b013e318245287d.

Jack Jr., C.R., Knopman, D.S., Weigand, S.D., Wiste, H.J., Vemuri, P., Lowe, V., Kantarci, K., Gunter, J.L., Senjem, M.L., Ivnik, R.J., Roberts, R.O., Rocca, W.A., Boeve, B.F., Petersen, R.C., 2012. An operational approach to National Institute on Aging-Alzheimer's Association criteria for preclinical Alzheimer disease. Ann. Neurol. 71, 765–775. http://dx.doi.org/10.1002/ana.22628.

Jagust, W.J., Landau, S.M., Alzheimer's Disease Neuroimaging, I, 2012. Apolipoprotein E, not fibrillar beta-amyloid, reduces cerebral glucose metabolism in normal aging. J. Neurosci. 32, 18227–18233. http://dx.doi.org/10.1523/JNEUROSCI.3266-12.2012.

Jagust, W.J., Bandy, D., Chen, K., Foster, N.L., Landau, S.M., Mathis, C.A., Price, J.C., Reiman, E.M., Skovronsky, D., Koeppe, R.A., 2010. The Alzheimer's Disease Neuroimaging Initiative positron emission tomography core. Alzheimers Dement. 6, 221–229. http://dx.doi.org/10.1016/j.jalz.2010.03.003.

Knopman, D.S., Jack Jr., C.R., Wiste, H.J., Weigand, S.D., Vemuri, P., Lowe, V., Kantarci, K., Gunter, J.L., Senjem, M.L., Ivnik, R.J., Roberts, R.O., Boeve, B.F., Petersen, R.C., 2012. Short-term clinical outcomes for stages of NIA-AA preclinical Alzheimer disease. Neurology 78, 1576–1582. http://dx.doi.org/10.1212/WNL.0b013e3182563bbe.

Knopman, D.S., Jack, C.R., Wiste, H.J., Weigand, S.D., Vemuri, P., Lowe, V.J., Kantarci, K., Gunter, J.L., Senjem, M.L., Mielke, M.M., Roberts, R.O., Boeve, B.F., Petersen, R.C., 2013. Selective Worsening of brain injury biomarker abnormalities in cognitively normal elderly persons with beta-Amyloidosis. JAMA Neurol. 70, 1030–1038. http://dx.doi.org/10.1001/jamaneurol.2013.182.

La Rue, A., Hermann, B., Jones, J.E., Johnson, S., Asthana, S., Sager, M.A., 2008. Effect of parental family history of Alzheimer's disease on serial position profiles. Alzheimers Dement. 4, 285–290. http://dx.doi.org/10.1016/j.jalz.2008.03.009.

Landau, S.M., Mintun, M.A., Joshi, A.D., Koeppe, R.A., Petersen, R.C., Aisen, P.S., Weiner, M.W., Jagust, W.J., Alzheimer's Disease Neuroimaging, I, 2012. Amyloid deposition, hypometabolism, and longitudinal cognitive decline. Ann. Neurol. 72, 578–586. http://dx.doi.org/10.1002/ana.23650.

Lim, Y.Y., Ellis, K.A., Pietrzak, R.H., Ames, D., Darby, D., Harrington, K., Martins, R.N., Masters, C.L., Rowe, C., Savage, G., Szoeke, C., Villemagne, V.L., Maruff, P., 2012. Stronger effect of amyloid load than APOE genotype on cognitive decline in healthy older adults. Neurology 79, 1645–1652. http://dx.doi.org/10.1212/WNL.0b013e31826e9ae6.

Logan, J., Fowler, J.S., Volkow, N.D., Wang, G.J., Ding, Y.S., Alexoff, D.L., 1996. Distribution volume ratios without blood sampling from graphical analysis of PET data. J. Cereb. Blood Flow Metab. 16, 834–840. http://dx.doi.org/10.1097/00004647-199609000-00008.

Lopresti, B.J., Klunk, W.E., Mathis, C.A., Hoge, J.A., Ziolko, S.K., Lu, X., Meltzer, C.C., Schimmel, K., Tsopelas, N.D., DeKosky, S.T., Price, J.C., 2005. Simplified quantification of Pittsburgh Compound B amyloid imaging PET studies: a comparative analysis. J. Nucl. Med. 46, 1959–1972 doi:46/12/1959 [pii].

Lowe, V.J., Kemp, B.J., Jack Jr., C.R., Senjem, M., Weigand, S., Shiung, M., Smith, G., Knopman, D., Boeve, B., Mullan, B., Petersen, R.C., 2009. Comparison of 18F-FDG and PiB PET in cognitive impairment. J. Nucl. Med. 50, 878–886. http://dx.doi.org/10.2967/jnumed.108.058529.

Maldjian, J.A., Laurienti, P.J., Kraft, R.A., Burdette, J.H., 2003. An automated method for neuroanatomic and cytoarchitectonic atlas-based interrogation of fMRI data sets. Neuroimage 19, 1233–1239.

Mathis, C.A., Kuller, L.H., Klunk, W.E., Snitz, B.E., Price, J.C., Weissfeld, L.A., Rosario, B.L., Lopresti, B.J., Saxton, J.A., Aizenstein, H.J., McDade, E.M., Kamboh, M.I., Dekosky, S.T., Lopez, O.L., 2013. In vivo assessment of amyloid-beta deposition in nondemented very elderly subjects. Ann. Neurol. 73, 751–761. http://dx.doi.org/10.1002/ana.23797.

Mielke, M.M., Wiste, H.J., Weigand, S.D., Knopman, D.S., Lowe, V.J., Roberts, R.O., Geda, Y.E., Swenson-Dravis, D.M., Boeve, B.F., Senjem, M.L., Vemuri, P., Petersen, R.C., Jack Jr., C.R., 2012. Indicators of amyloid burden in a population-based study of cognitively normal elderly. Neurology 79, 1570–1577. http://dx.doi.org/10.1212/WNL.0b013e31826e2696.

Morris, J.C., Roe, C.M., Xiong, C., Fagan, A.M., Goate, A.M., Holtzman, D.M., Mintun, M.A., 2010. APOE predicts amyloid-beta but not tau Alzheimer pathology in cognitively normal aging. Ann. Neurol. 67, 122–131. http://dx.doi.org/10.1002/ana.21843.

Mosconi, L., Brys, M., Switalski, R., Mistur, R., Glodzik, L., Pirraglia, E., Tsui, W., De Santi, S., de Leon, M.J., 2007. Maternal family history of Alzheimer's disease predisposes to reduced brain glucose metabolism. Proc. Natl. Acad. Sci. U.S.A 104, 19067–19072. http://dx.doi.org/10.1073/pnas.0705036104.

Mosconi, L., Mistur, R., Switalski, R., Brys, M., Glodzik, L., Rich, K., Pirraglia, E., Tsui, W., De Santi, S., de Leon, M.J., 2009. Declining brain glucose metabolism in normal individuals with a maternal history of Alzheimer disease. Neurology 72, 513–520. http://dx.doi.org/10.1212/01.wnl.0000333247.51383.43.

Mosconi, L., Rinne, J.O., Tsui, W.H., Berti, V., Li, Y., Wang, H., Murray, J., Scheinin, N., Nagren, K., Williams, S., Glodzik, L., De Santi, S., Vallabhajosula, S., de Leon, M.J., 2010. Increased fibrillar amyloid-{beta} burden in normal individuals with a family history of late-onset Alzheimer's. Proc. Natl. Acad. Sci. U.S.A 107, 5949–5954. http://dx.doi.org/10.1073/pnas.0914141107.

Mosconi, L., Rinne, J.O., Tsui, W.H., Murray, J., Li, Y., Glodzik, L., McHugh, P., Williams, S., Cummings, M., Pirraglia, E., Goldsmith, S.J., Vallabhajosula, S., Scheinin, N., Viljanen, T., Nagren, K., de Leon, M.J., 2013. Amyloid and metabolic positron emission tomography imaging of cognitively normal adults with Alzheimer's parents. Neurobiol. Aging 34, 22–34. http://dx.doi.org/10.1016/j.neurobiolaging.2012.03.002.

Nichols, L.M., Masdeu, J.C., Mattay, V.S., Kohn, P., Emery, M., Sambataro, F., Kolachana, B., Elvevag, B., Kippenhan, S., Weinberger, D.R., Berman, K.F., 2012. Interactive effect of apolipoprotein e genotype and age on hippocampal activation during memory processing in healthy adults. Arch. Gen. Psychiatry 69, 804–813. http://dx.doi.org/10.1001/archgenpsychiatry.2011.1893.

Oh, H., Habeck, C., Madison, C., Jagust, W., 2012. Covarying alterations in Abeta deposition, glucose metabolism, and gray matter volume in cognitively normal elderly. Hum. Brain Mapp. http://dx.doi.org/10.1002/hbm.22173.

Okonkwo, O.C., Xu, G., Dowling, N.M., Bendlin, B.B., Larue, A., Hermann, B.P., Koscik, R., Jonaitis, E., Rowley, H.A., Carlsson, C.M., Asthana, S., Sager, M.A., Johnson, S.C., 2012a. Family history of Alzheimer disease predicts hippocampal atrophy in healthy middle-aged adults. Neurology 78, 1769–1776. http://dx.doi.org/10.1212/WNL.0b013e3182583047.

Okonkwo, O.C., Xu, G., Oh, J.M., Dowling, N.M., Carlsson, C.M., Gallagher, C.L., Birdsill, A.C., Palotti, M., Wharton, W., Hermann, B.P., Larue, A., Bendlin, B.B., Rowley, H.A., Asthana, S., Sager, M.A., Johnson, S.C., 2012b. Cerebral blood flow is diminished in asymptomatic middle-aged adults with maternal history of Alzheimer's disease. Cereb. Cortex. http://dx.doi.org/10.1093/cercor/bhs381.

Palop, J.J., Mucke, L., 2010. Amyloid-beta-induced neuronal dysfunction in Alzheimer's disease: from synapses toward neural networks. Nat. Neurosci. 13, 812–818. http://dx.doi.org/10.1038/nn.2583.

Price, J.C., Klunk, W.E., Lopresti, B.J., Lu, X., Hoge, J.A., Ziolko, S.K., Holt, D.P., Meltzer, C.C., Dekosky, S.T., Mathis, C.A., 2005. Kinetic modeling of amyloid binding in humans using PET imaging and Pittsburgh Compound-B. J. Cereb. Blood Flow Metab. 25, 1528–1547.

Reiman, E.M., Quiroz, Y.T., Fleisher, A.S., Chen, K., Velez-Pardo, C., Jimenez-Del-Rio, M., Fagan, A.M., Shah, A.R., Alvarez, S., Arbelaez, A., Giraldo, M., Acosta-Baena, N., Sperling, R.A., Dickerson, B., Stern, C.E., Tirado, V., Munoz, C., Reiman, R.A., Huentelman, M.J., Alexander, G.E., Langbaum, J.B., Kosik, K.S., Tariot, P.N., Lopera, F., 2012. Brain imaging and fluid biomarker analysis in young adults at genetic risk for autosomal dominant Alzheimer's disease in the presenilin 1 E280A kindred: a case-control study. Lancet Neurol. 11, 1048–1056. http://dx.doi.org/10.1016/S1474-4422(12)70228-4.

Ridgway, G.R., Henley, S.M., Rohrer, J.D., Scahill, R.I., Warren, J.D., Fox, N.C., 2008. Ten simple rules for reporting voxel-based morphometry studies. Neuroimage 40, 1429–1435. http://dx.doi.org/10.1016/j.neuroimage.2008.01.003.

Rodrigue, K.M., Kennedy, K.M., Devous Sr., M.D., Rieck, J.R., Hebrank, A.C., Diaz-Arrastia, R., Mathews, D., Park, D.C., 2012. beta-Amyloid burden in healthy aging: regional distribution and cognitive consequences. Neurology 78, 387–395. http://dx.doi.org/10.1212/WNL.0b013e318245d295.

Rowe, C.C., Ellis, K.A., Rimajova, M., Bourgeat, P., Pike, K.E., Jones, G., Fripp, J., Tochon-Danguy, H., Morandeau, L., O'Keefe, G., Price, R., Raniga, P., Robins, P., Acosta, O., Lenzo, N., Szoeke, C., Salvado, O., Head, R., Martins, R., Masters, C.L., Ames, D., Villemagne, V.L., 2010. Amyloid imaging results from the Australian Imaging, Biomarkers and Lifestyle (AIBL) study of aging. Neurobiol. Aging 31, 1275–1283. http://dx.doi.org/10.1016/j.neurobiolaging.2010.04.007.

Sager, M.A., Hermann, B., La Rue, A., 2005. Middle-aged children of persons with Alzheimer's Disease: APOE genotypes and cognitive function in the Wisconsin Registry for Alzheimer's Prevention. J. Geriatr. Psychiatry Neurol. 18, 245–249.

Sperling, R.A., Aisen, P.S., Beckett, L.A., Bennett, D.A., Craft, S., Fagan, A.M., Iwatsubo, T., Jack Jr., C.R., Kaye, J., Montine, T.J., Park, D.C., Reiman, E.M., Rowe, C.C., Siemers, E., Stern, Y., Yaffe, K., Carrillo, M.C., Thies, B., Morrison-Bogorad, M., Wagster, M.V., Phelps, C.H., 2011. Toward defining the preclinical stages of Alzheimer's disease: recommendations from the National Institute on Aging-Alzheimer's Association workgroups on diagnostic guidelines for Alzheimer's disease. Alzheimer's Dement. 7, 280–292. http://dx.doi.org/10.1016/j.jalz.2011.03.003.

Sperling, R.A., Johnson, K.A., Doraiswamy, P.M., Reiman, E.M., Fleisher, A.S., Sabbagh, M.N., Sadowsky, C.H., Carpenter, A., Davis, M.D., Lu, M., Flitter, M., Joshi, A.D., Clark, C.M., Grundman, M., Mintun, M.A., Skovronsky, D.M., Pontecorvo, M.J., 2013. Amyloid deposition detected with florbetapir F 18 ((18) F-AV-45) is related to lower episodic memory performance in clinically normal older individuals. Neurobiol. Aging 34, 822–831. http://dx.doi.org/10.1016/j.neurobiolaging.2012.06.014.

Swerdlow, R.H., 2011. Brain aging, Alzheimer's disease, and mitochondria. Biochim. Biophys. Acta 1812, 1630–1639. http://dx.doi.org/10.1016/j.bbadis.2011.08.012.

Wilson, A.A., Garcia, A., Jin, L., Houle, S., 2000. Radiotracer synthesis from [(11)C]-iodomethane: a remarkably simple captive solvent method. Nucl. Med. Biol. 27, 529–532.

Worsley, K.J., Taylor, J.E., Tomaiuolo, F., Lerch, J., 2004. Unified univariate and multivariate random field theory. Neuroimage 23 (Suppl 1), S189–S195. http://dx.doi.org/10.1016/j.neuroimage.2004.07.026.

Xiong, C., Roe, C.M., Buckles, V., Fagan, A., Holtzman, D., Balota, D., Duchek, J., Storandt, M., Mintun, M., Grant, E., Snyder, A.Z., Head, D., Benzinger, T.L., Mettenburg, J., Csernansky, J., Morris, J.C., 2011. Role of family history for Alzheimer biomarker abnormalities in the adult children study. Arch. Neurol. 68, 1313–1319. http://dx.doi.org/10.1001/archneurol.2011.208.